Cumulative Conformance Count Charts with Variable Sample Sizes

Y. K. Chen and C. Y. Chen

Abstract—**Cumulative count of conforming (CCC) chart has been shown effective for high-yield processes with very low fraction of nonconforming items. Traditional CCC chart assumes the products from a process are inspected item by item. Recently, the CCC chart was generalized to conform to the industrial practice where items are inspected sample by sample without according to the production order. Different from the traditional chart, the generalized CCC chart monitors the cumulative count of samples until a nonconforming sample is encountered. In order to improve the power of the generalized CCC chart to detect process changes, this study applied the control scheme of variable sample size (VSS) to the generalized CCC chart. The average time to signal (ATS) process change of the proposed chart was derived by Markov chain approach and taken as performance measure to evaluate its statistical efficiency. Performance comparisons between the proposed chart and generalized CCC chart are made to evaluate its usefulness.**

Index Terms—**Cumulative conformance count, variable sample size, markov chain.**

I. Introduction

The control chart is one of the primary statistical process control tool for improving and maintaining quality and productivity of modern manufacturing industries. The use of a control chart is to detect the assignable causes in the process as early as possible and help to remove them. Adaptive control charts are ones with an adaptive control scheme that allow at least one of their parameters (sampling size, sampling interval, and control limits) to adapt, depending on the indication of sample statistic on the chart. The use of adaptive control schemes is to improve the time required for detecting process changes and reduce its cost. Up to now, most of the works on adaptive control charts focus on the $\overline{X}$ charts. The variable sampling intervals (VSI) $\overline{X}$ chart was initiated by Reynolds, Amin, Arnold & Nachlas [1]. Subsequently, Reynolds [2], Amin & Hemasinha [3] and Amin & Miller [4] studied in depth the properties of the VSI $\overline{X}$ charts. Prabhu, Runger & Keats [5] and Costa [6] studied the properties of the variable sample size (VSS) $\overline{X}$ charts. The properties of the charts with variable sample size and

Y. K. Chen is with Department of Distribution Management, National Taichung University of Science and Technology, 129, Sec 3, Sanmin Rd, Taichung, Taiwan (e-mail: ykchen@ nutc.edu.tw).

C. Y. Chen is with Department of Electronic Engineering, National Yunlin University of Science & Technolgy, 123, Sec 3, University Rd, Douliu, Yunlin, Taiwan (e-mail: author@lamar. colostate.edu).

variable sampling interval (VSSI) were further studied in many papers (e.g., [7]-[9]). The use of adaptive parameters has also applied to other variable charts, such as the EWMA charts [10], CUSUM charts [11], $\overline{X} - R$ charts [12], and multivariate charts [13], [14].

While there are several studies on adaptive control chart for variables, it is seldom to find the studies on adaptive control chart for attributes. However, it has been shown that the control scheme of adapting parameters is capable of improving the performance of the control chart for attributes as well (e.g., [15]-[19]).

Due to the rapid growth of automated technologies, many production processes today are producing a very low level of nonconforming items. In view of this, the cumulative conformance count (CCC) chart has received many attentions from the industry (e.g., [20]-[22]). Traditionally, it is assumed that the products from a process are inspected item by item or sequentially in the order of production when implementing the CCC chart. However, in view of a large production volume, an economy of scale or easy in group inspection, there are practical situations where products from a process are inspected sample by sample or lot by lot, without preserving the original ordering of production [23]. In such circumstances, the traditional CCC chart is no longer applicable. To adapt to this case, Zhang et al.[23] proposed a generalized CCC chart to monitor the cumulative number of samples until a nonconforming sample is encountered. The generalized CCC chart can reduce to the traditional CCC chart if the sample size equals 1.

In this paper, we extend the variable sampling scheme to the generalized CCC chart. Note that in the CCC chart each time a sample is inspected one may not obtain a data point of the chart statistic as in the traditional Shewhart-type chart. Therefore, we assume sampling at fixed times and only discuss the generalized CCC chart with the VSS scheme by administrative considerations.

II. The VSS-CCC Charts

Consider a situation where products from a process are inspected sample by sample without according to the original ordering of production. We name a sample nonconforming if it contains one or more nonconforming items and conforming if it contains nonconforming items. Assume the fractional nonconforming of the process is p and the sample size for each sampling inspection is n.

Then the probability that a sample is nonconforming in in-control state is given by
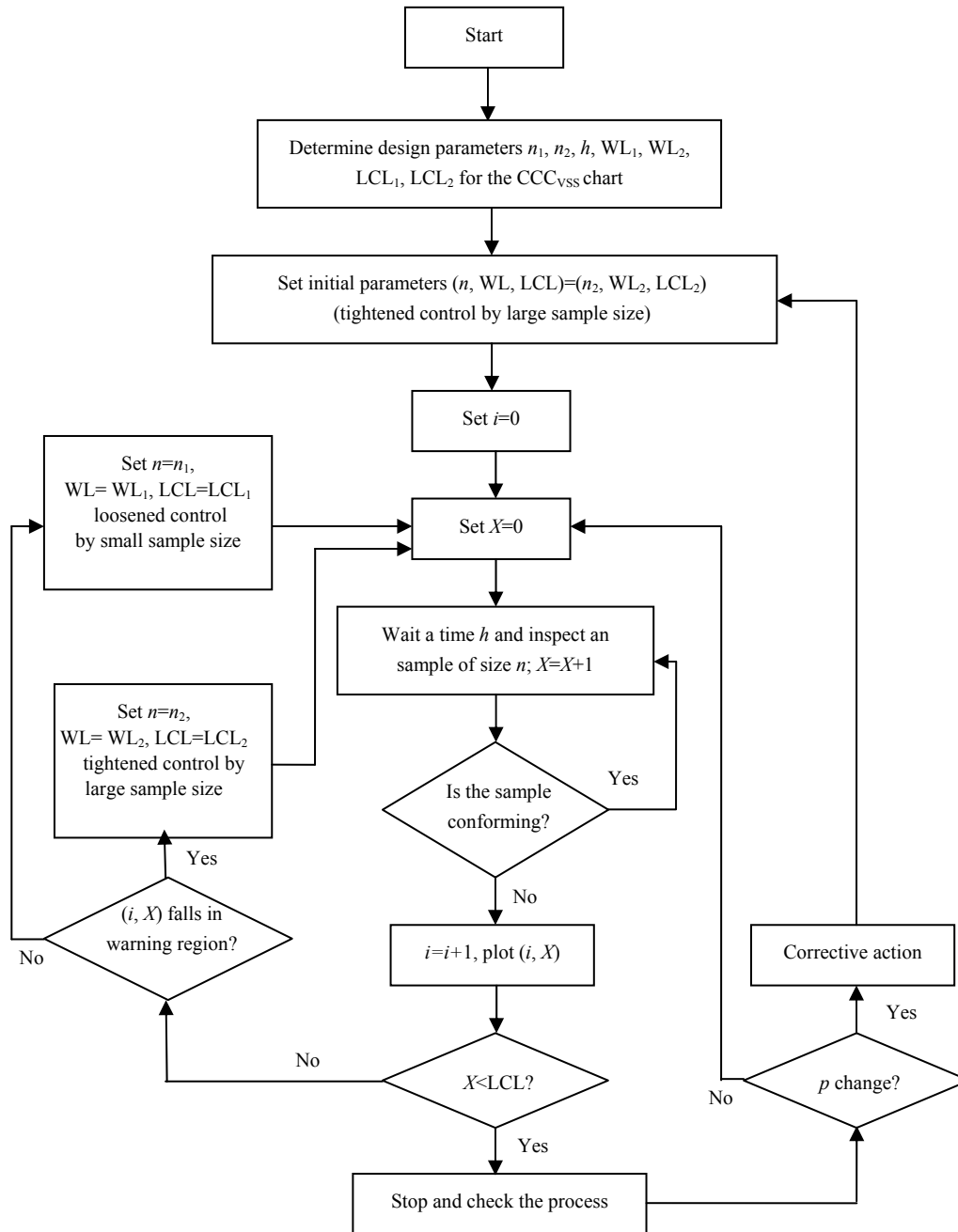
$$p_n = 1 - (1 - p)^n \qquad (1)$$

Fig. 1. The charting and decision procedure for the CCC_{VSS} chart.

For a high-yield manufacturing environment, the values of p is assumed very small and thus p_n is also small. Let X be the number of samples inspected until a nonconforming sample is detected. Then X is coming from a geometric distribution with distribution function $F(x)$:

$$F(x) = 1 - (1-p)^{nx}, \quad x = 1, 2, \cdots \quad (2)$$

When a generalized CCC chart is applied to monitor the process parameter p, the values of X are calculated and plotted over time on the chart with the upper control limit (UCL) and lower control limit (LCL). In a generalized CCC chart, X plotting below the LCL indicates a possible deterioration of the process, while X plotting beyond the UCL indicates the process is better and the fraction of nonconformance is smaller, therefore, we shall only focus on a low-sided chart because it is usually more concerned in practice. Besides, as the geometric distribution is highly skewed when the parameters p_n is very small, the chart employs probability control limits instead of using the traditional three sigma as control limits to increase its efficiency [24]. Let α be an acceptable rate of false alarm, according to the suggestion of probability control limits the LCL can be determined by $\Pr\{X < \text{LCL}\} = \alpha$ (or $1 - (1-p)^{n \times (\text{LCL}-1)} = \alpha$). As the geometric distribution is discrete, the control limit could be rounded to integers and calculated by.

$$LCL = [\frac{1}{n} \times \frac{ln(1-\alpha)}{ln(1-p)}] \tag{3}$$

where [y] stands for the largest integer not greater than y. The true false alarm rate α' getting from the rounded control limit may be not exactly equal to α, but it is extremely close when p is very small [18].

For the generalized CCC chart, the time between successively inspected samples is treated as the sampling interval (saying h). The sample size, sampling interval length, and control limit are fixed without any change through the process. The generalized CCC chart can reduce to standard one if the sample size is 1, i.e., the case that items are inspected one by one in the order of production.

The VSS CCC chart (namely the CCC_{VSS} chart) is a modification of the generalized CCC chart. Let n_1 and n_2 be the minimum and maximum sample sizes, respectively, such that $n_1 \leq n \leq n_2$ while keeping the sampling interval fixed at h for the administration consideration. The decision to switch between the maximum and minimum sample size depends on position of the prior sample point on the control chart. If the prior sample point falls in the safe region, the minimum sample size n_1 will be used for the current sample point; if the prior sample point falls in the warning region, the maximum sample size n_2 will be used for the current sample point. Finally, if the prior sample point falls in the action region, then the process is considered out-of-control. Here the safety, warning and action regions are given by the warning limit(WL) and the lower control limit (LCL): safety region is given by (WL_j, ∞), warning region is given by $(LCL_j, WL_j]$, and the action region is given by $(0, LCL_j]$, where $j = 1$ if the prior sample point comes from the small sample, whereas $j = 2$ if the prior sample point comes from the large sample. Consequently, $WL_1 \geq WL_2$ and $LCL_1 \geq LCL_2$. For the sake of simplicity, we assume WL_j is selected such that

$$\begin{aligned} \tau &= \Pr\{LCL_1 < X \leq WL_1\}/\Pr\{LCL_1 < X < \infty\} \\ &= \Pr\{LCL_2 < X \leq WL_2\}/\Pr\{LCL_2 < X < \infty\} \end{aligned} \tag{4}$$

where τ is the probability allocation determined by users.

As the warning limit and lower control limit are varied depending on the value of X, we follow the idea of Costa [25] to construct a control chart with two scales: one on left hand side and the other on the right hand side. The point obtained from the minimum sample is plotted according to the left scale, whereas the one obtained from the maximum sample is plotted according to the right scale. Because the left scale is not proportional to the right scale, we further break the left scale referring to Costa [25] and plot the point inside the right region. In this way, the effort to monitor a process with the CCC_{VSS} chart or with the generalized CCC chart is almost the same.

Fig. 1 shows the charting and decision procedure for the CCC_{VSS} chart. To give additional protection against problems that arises during start-up, the initial sample size is set to be the maximum sample size n_2, and thus the warning limit and lower control limit are WL_2 and LCL_2 respectively to tighten the control. The charting and decision procedure is similar to that of the generalized chart except that the adaptive control: tightened or loosened depends on the position the current point falls.

III. PERFORMANCE MEASURE

Average time to signal (ATS) is the most commonly used measure to evaluate the statistical performance of different control charts when the lengths of time interval between two successive sample points are not fixed and equal for the compared charts. When the process is in-control, the larger the value for ATS the lower the false alarm rate; whereas when the process is out-of-control, the smaller the value for ATS, the quicker the speed it takes the chart to detect the increase in the fractional nonconforming.

Due to the memoryless property of the geometric distribution, the ATS performance for the CCC_{VSS} chart can be determined by the Markov chain approach [26]. At each sample point, one of the following states can be reached: State 1: $X \in$ safety region, State 2: $X \in$ warning region, and State 3: $X \in$ action region. States 1 and 2 are transient states and State 3 is an absorbing state. The transition probability matrix is given by

$$\mathbf{P} = \begin{bmatrix} p_{11} & p_{12} & p_{13} \\ p_{21} & p_{22} & p_{23} \\ 0 & 0 & 1 \end{bmatrix} \tag{5}$$

Where

$$\begin{aligned} p_{11} &= \Pr\{X > WL_1\} = 1 - \Pr\{X \leq WL_1\} \\ &= 1 - [1 - (1-p)^{n_1 \times WL_1}] = (1-p)^{n_1 \times WL_1}; \\ p_{12} &= \Pr\{LCL_1 < X \leq WL_1\} \\ &= (1-p)^{n_1 \times LCL_1} - (1-p)^{n_2 \times WL_1}; \\ p_{13} &= 1 - p_{11} - p_{12}; \\ p_{21} &= \Pr\{X > WL_2\} = (1-p)^{n_2 \times WL_2}; \\ p_{22} &= \Pr\{LCL_2 < X \leq WL_2\} \\ &= (1-p)^{n_2 \times LCL_2} - (1-p)^{n_2 \times WL_2}; \\ p_{23} &= 1 - p_{21} - p_{22}. \end{aligned}$$

Note that the notation p in above formulae stands for the fractional nonconforming of the process: $p = p_0$ means the process is in-control while $p = p_1$ means the process is out-of-control. By the elementary properties of the Markov chain,

$$ATS = \mathbf{r}(\mathbf{I} - \mathbf{Q})^{-1}\mathbf{t} \tag{6}$$

where $\mathbf{r} = (r_1, r_2)$ is the vector of initial probability for states 1 and 2 such that $r_1 + r_2 = 1$ (In this paper, the vector $\mathbf{r}$ is set as (0, 1) to provide a tightening control to prevent problems that are encountered during start-up); $\mathbf{I}$ is the identity matrix of order 2; $\mathbf{Q}$ is the transition matrix $\mathbf{P}$ where elements

associated with the absorbing state are deleted; and $\mathbf{t} = \left(\dfrac{h}{p_{n_1}}, \dfrac{h}{p_{n_2}} \right)$ is the vector of average time required to encounter the next nonconforming sample when arriving at one of the two transient states 1 and 2. Consequently,

$$(\mathbf{I} - \mathbf{Q})^{-1} = \begin{bmatrix} \dfrac{1 - p_{22}}{A} & \dfrac{p_{12}}{A} \\ \dfrac{p_{21}}{A} & \dfrac{1 - p_{11}}{A} \end{bmatrix} \qquad (7)$$

where $A = (1 - p_{11})(1 - p_{22}) - p_{21}p_{12}$.

For the generalized CCC chart, the ATS can be reached by letting $n_1 = n_2 = n_0$, $\text{WL}_1 = \text{LCL}_1$, $\text{WL}_2 = \text{LCL}_2$, and $\text{LCL}_1 = \text{LCL}_2$, which imply $p_{12} = p_{22} = 0$ and $p_{11} = p_{21}$.

IV. CHART DESIGNING

In order to evaluate the performance of the CCC_{VSS} chart, it is necessary to design the CCC_{VSS} chart to match the generalized CCC chart with equal conditions. That is, they require the same average number of items inspected (ANI) until the appearance of a false alarm and the same in-control ATS (denoted by ATS_0) to ensure the process is under control for most of the time. To do so, we first give the value to one of n_1 and n_2, and seek the values for another and probability allocation τ to obtain an average sample size n_0 when the process is in-control:

$$n_1(1 - \tau) + n_2\tau = n_0 \qquad (8)$$

This requirement is to ensure the averaged sample size are the same for compared charts. As the lengths of sampling interval for both charts are fixed and identical. If the parameters of n_1, n_2, and τ are specified to make sure both charts have the equal ATS_0, then the compared charts will have the same ANI until the appearance of a false alarm. Accordingly, the procedure for designing the CCC_{VSS} chart to match the generalized CCC chart is summarized as follows:

Step1. Given the values for α, h, n_0 and p_0.

Step2. Choose the value for n_1 ($\leq n_0$) and determine the rounded maximum control limit LCL_1 by (3):

$$\text{LCL}_1 = [\dfrac{1}{n_1} \times \dfrac{ln(1-\alpha)}{ln(1-p_0)}]. \qquad (9)$$

Note that $\alpha > p_0$ is required to get a meaningful LCL_1 (i.e., $\text{LCL}_1 \geq 1$).

Step3. Determine the value for n_2 ($\geq n_0$) such that both charts have almost the same in-control ATS (denoted by ATS_0). The search for n_2 can be conducted as follows.

  Step3-1. Let n_2 start with n_0.

  Step3-2. Determine the rounded minimum control limit

LCL_2 by

$$\text{LCL}_2 = [\dfrac{1}{n_2} \times \dfrac{ln(1-\alpha)}{ln(1-p_0)}] \qquad (10)$$

while determine the probability allocation τ by

$$\tau = (n_0 - n_1)/(n_2 - n_1). \qquad (11)$$

Step3-3. By means of equation (4) determine the rounded warning limits:

$$\text{WL}_j = [\dfrac{ln(1-\tau) + n_j \times \text{LCL}_j \times ln(1-p_0)}{n_j \times ln(1-p_0)}], \ j = 1, 2 \quad (12)$$

Step3-4. Calculate the ATS_0 for both charts by equation (6). If the values are almost the same then stop. Otherwise, let $n_2 = n_2 + 1$ and go to Step 3-2 until n_2 attains the acceptable upper bound.

Due to the rounded warning /control limits to integers, the conditions (9), (10) and (12) may be not exactly held. However, it should be achieved when p_0 is very small.

V. COMPARISONS BETWEEN CHARTS

Once the CCC_{VSS} chart is designed to match the generalized CCC chart with equal in-control conditions, the out-of-control ATS performance (denoted as ATS_1) will be calculated by (6) to evaluate the efficiency of the CCC_{VSS} chart, which is defined as the percentage of improvement (PI) in ATS_1:

$$\text{PI} = \dfrac{\text{ATS}_1(\text{CCC chart}) - \text{ATS}_1(\text{CCC}_{\text{VSS}}\ \text{chart})}{\text{ATS}_1(\text{CCC chart})} \times 100\% \quad (13)$$

when PI is less than or equal to 0, the ATS_1 of the generalized CCC chart is less than or equal to that of the CCC_{VSS} chart, which means the CCC_{VSS} chart is inefficient. Oppositely, when PI is greater than 0, the ATS_1 of the generalized CCC chart is greater than that of the CCC_{VSS} chart, which means the CCC_{VSS} chart is efficient. The larger the PI, the better the efficiency of the CCC_{VSS} chart.

Let $\alpha = 0.005$, $h = 1.0$, $p_0 = 5 \times 10^{-6}$, we compare the matched CCC_{VSS} chart and the generalized CCC chart in terms of the percentage of improvement (PI) in ATS_1 for the following cases: $n_0 = 10$, 15 and 20. In each case, the value for n_1 is given to find the value for n_2 (e.g., in the case of $n_0 = 10$, when the value of n_1 is given by 1, the value of n_2 is 503 to match the CCC_{VSS} chart with the generalized CCC chart.) A simple computer program for EVOLOVER4.0 was written to search for n_2. Table I provides the comparison

results for different degrees of changes in the fractional nonconforming.

TABLE I: VALUES OF PI (%) BY THE CCC_{VSS} CHART UNDER α=0.005, h=1 AND p_0=5×10^{-6}

n_0	(n_1, n_2)	Shifts (= p_1/p_0)											
		1.0	2.0	3.0	4.0	5.0	6.0	7.0	8.0	9.0	10	20	50
10	(1, 503)	0	2	2	3	4	4	5	6	6	7	14	36
	(5, 502)	0	1	1	1	1	2	2	2	2	3	6	15
	(9, 403)	0	0	0	0	0	0	1	1	1	1	2	4
15	(1, 509)	0	4	5	6	7	8	9	11	12	13	25	57
	(7, 503)	0	2	3	3	4	4	5	6	6	7	12	30
	(14, 352)	0	1	1	1	1	1	1	1	1	1	1	2
20	(1, 510)	0	4	5	7	9	10	12	14	15	17	33	69
	(10, 502)	0	1	2	4	5	6	7	8	9	10	19	39
	(19, 82)	0	1	2	3	4	5	5	6	7	8	16	39

From Table I, it can be found that

(1) The greater the shift in the fractional nonconforming p_1/p_0, the larger the value for PI, and the more efficient the CCC_{VSS} chart as compared with the generalized CCC chart.

(2) The greater the difference between the lengths of n_1 and n_2, the larger the value for PI, and the more efficient the CCC_{VSS} chart as compared with the generalized CCC chart.

(3) The larger the value for averaged sample size n_0, the larger the value for PI, and the more efficient the CCC_{VSS} chart as compared with the generalized CCC chart.
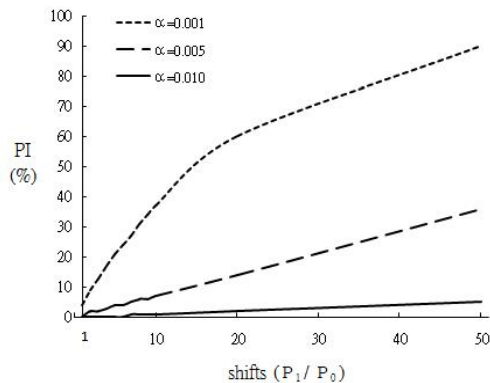

Fig. 2. The trend of PI (%) values for different false alarm rates.
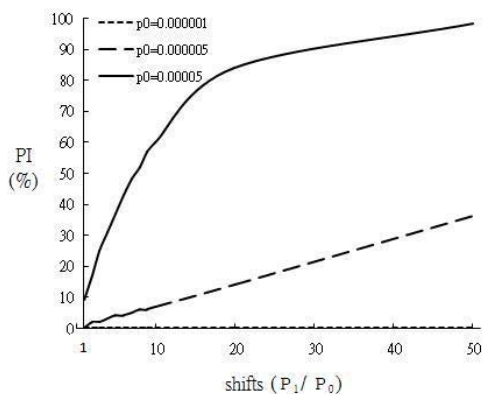

Fig. 3. The trend of PI (%) values for different in-control fractional nonconforming.

To further investigate the effects of the averaged false alarm rate (α) and the fractional nonconforming (p_0) on the trend of the PI (%) values for different process shifts, we fixed $n_0 = 10$ and $n_1 = 1$ in accordance with the finding from Table I, and only changed one of α and p_0 at a time. Fig. 2 and 3 depict the trends of PI (%) against different false alarm rate and original fractional nonconforming, respectively. As we can see, the trend of PI (%) values is affected by both of the false alarm rate and original fractional nonconforming: the value for PI increases as the false alarm rate decreases or as the original fractional nonconforming increase. In other words, the CCC_{VSS} chart is more efficient when the false alarm rate is small or when the original fractional nonconforming is not extremely small.

VI. INDUSTRIAL EXAMPLE

Assume an injection molding process that produces the micro-prism array of optical element by way of the three stages: filling, packing, packing and cooling. The surface roughness of the product directly impacts its surface quality. Thus, the mould's should be polished to ensure it within the specification. Once the parameter selection is complete and the machinery is stabilized, the process can move on to fully automated production. In such a manufacturing environment, the yield of the process is very high. Generally, the fractional nonconforming p_0 is at the level of $5×10^{-6}$. For most of time the process stays in the in-control state, but occasionally the fractional nonconforming shifts from the original level. The items are manufactured lot by lot. The lot size is 1200 items and the cycle time for each item is about 3 seconds, so it needs about two hours for a lot (h=1.0). Due to economy of scale a sample of size 20 (n_0 =20) is taken from each lot and inspected without preserving the original ordering of production. In such circumstance, a generalized CCC chart is employed to monitor the cumulative number of samples X until a nonconforming sample is met. The X values are plotted on the chart with lower control limit placed at $LCL = [n_0^{-1} \times ln(1-\alpha)/ln(1-p_0)] = 50$.

As the speed with the generalized CCC chart to detect the process shift is low, the process engineer is planning to monitor the process by adding a VSS feature to the generalized CCC chart. The new plan puts a warning limit in the CCC_{VSS} chart to identify when to shift from one sample

size to another (see Fig. 4). By choosing $n_1 = 1$, the value for n_2 is determined by 510 to match the generalized CCC chart. Meanwhile, this plan varies the warning limit WL and the lower control limit LCL between two values: (8461, 15) for (WL_1, WL_2), (1002, 1) for (LCL_1, LCL_2). Accordingly, if the current X value falls into the safety region, the minimum sample size of one item will be used until the next nonconforming sample appears; oppositely, if the current X value falls into the warning region, the maximum sample size of 510 items will be used until the next nonconforming sample appears. The process is stopped if the X value falls into the action region.
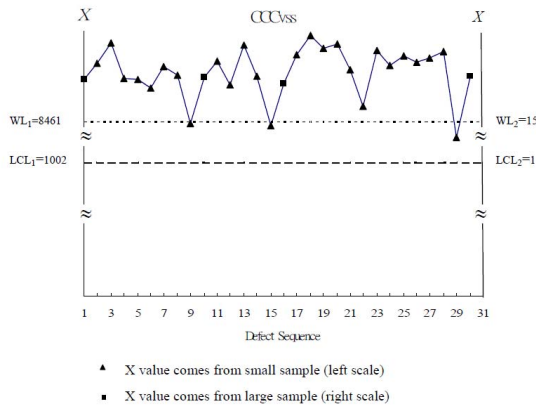

Fig. 4. The CCC_{VSS} chart from the example.

TABLE II: A SET OF DATA FROM THE EXAMPLE

Defect Sequence	X	R/L scale ?	Defect Sequence	X	R/L scale ?
1	81132	R	16	64745	R
2	190696	L	17	290503	L
3	532190	L	18	786173	L
4	86199	L	19	410382	L
5	79594	L	20	502335	L
6	50787	L	21	130186	L
7	162332	L	22	19783	L
8	98322	L	23	356576	L
9	8104	L	24	168452	L
10	92770	R	25	274622	L
11	211254	L	26	202861	L
12	60761	L	27	252520	L
13	485795	L	28	343616	L
14	96833	L	29	4011	L
15	7133	L	30	98110	R

Table II shows a set of data from the process. The CCC_{VSS} chart based on the data set is shown in Fig. 4. The left scale in the chart with the warning limit of 8461 and lower control limit of 1002 is used when the X values obtained from small sample. On the other hand, the right scale with the warning limit of 15 and lower control limit of 1 is used for X values from large sample. The VSS feature improves the efficiency of the generalized CCC chart in terms of the out-of-control ATS performance. When the level of fractional nonconformance shifts from the original level to 5×10^{-5}, the ATS of the CCC_{VSS} chart in the plan is the 83% of that of the generalized CCC chart.

VII. CONCLUSION

Zhang et al. (2008) generalized the CCC charts to accommodate to situations where products are inspected sample by sample without preserving or according to the production ordering. This paper extended Zhang et al.'s work by adding the feature of VSS to the generalized CCC charts. Since it allows the sample size changeable depending on the indication of sample statistic on the chart, the CCC_{VSS} chart can detect increase in the nonconforming rate more quickly, and thus reduce the average count of nonconforming items from the process. In addition, the greater the increase in the fractional nonconforming, the greater the improvement on the performance of the generalized CCC charts by the matched CCC_{VSS} chart with equal in-control ATS. On the other hand, when the shift in the fractional nonconforming remains constant, the efficiency of CCC_{VSS} chart can be enhanced by increasing the difference between the sample sizes or by decreasing the false alarm rate.

REFERENCES

[1] M. R. Reynolds, JR, R. W. Amin, J. C. Arnold, and J. A. Nachlas, "$\bar{X}$ charts with variable sampling intervals," *Technometrics*, vol. 30, pp. 181-192, 1988.

[2] M. R. Reynolds, JR, "Evaluating properties of variable sampling interval control charts," *Sequential Analysis*, vol.14, pp. 59-97, 1995.

[3] R. W. Amin and R. Hemasinha, "The switching behavior of $\bar{X}$ charts with variable sampling intervals," *Communication in Statistics-Theory and Methods*, vol.22, pp. 2081-2102, 1993.

[4] R.W. Amin and R. W. Miller, "A robustness study of $\bar{X}$ charts with variable sampling intervals," *Journal of Quality Technology*, vol.25, pp.36-44, 1993.

[5] S. S. Prabhu, G. C. Runger, and J. B. Keats, "An adaptive sample size $\bar{X}$ chart," *International Journal of Production Research*, vol. 31, pp. 2895-2909, 1993.

[6] A. F. B. Costa, "$\bar{X}$ control chart with variable sample size," *Journal of Quality Technology*, vol. 26, pp.155-163, 1994.

[7] S. S. Prabhu, D. C. Montgomery, and G.C. Runger, "A combined adaptive sample size and sampling interval $\bar{X}$ control chart," *Journal of Quality Technology*, vol.26, pp.164-176, 1994.

[8] T. K. Das and V. Jain, "Economic design of dual-sampling-interval policies for charts with and without run rules," *IIE Transactions*, vol.29, pp.497-506, 1997.

[9] A. F. B. Costa, "$\bar{X}$ charts with variable sample sizes and sampling intervals," *Journal of Quality Technology*, vol. 29, pp.197-204, 1997.

[10] M. S. Saccucci, R. W. Amin, and J. M. Lucas, "Exponentially weighted moving average control schemes with variable sampling intervals," *Communications in Statistics-Simulation and Computation*, vol.21, pp.627-657, 1992.

[11] H. P. Annadi, J. B. Keats, G. C. Runger, and D. C. Montgomery, "An adaptive sample size cusum control chart," *International Journal of Production Research*, vol.33, pp.1605-1616, 1995.

[12] A. F. B. Costa, "Joint $\bar{X}$ and R control charts with variable parameters," *IIE Transactions*, vol. 30, pp. 505-514, 1998.

[13] F. Aparisi, "Hotelling's T^2 control chart with adaptive sample sizes," *International Journal of Production Research*, vol. 34, pp.2853-2862, 1996.

[14] Y. K. Chen and K. L. Hsieh, "Hotelling's T^2 Charts with Variable Sample Size and Control Limit," *European Journal of Operational Research*, vol.182, pp.1251-1262, 2007.

[15] T. S. Vaughan, "Variable sampling interval np process control chart," *Communications in Statistics-Theory and Method*, vol. 22, pp.147-167, 1993.

[16] E. K. Epprecht and A. F. B. Costa, "Adaptive sample size control charts for attributes," *Quality Engineering*, vol.13, pp.465-473, 2001.

[17] E. K. Epprecht, A. F. B. Costa, F. C. T. Mendes, " Adaptive control charts for attributes," *IIE Transactions*, vol.35, pp.567-582, 2003.

[18] J. Y. Liu, M. Xie, T. N. Goh, Q. H. Liu, and Z. H. Yang, "Cumulative count of conforming chart with variable sampling intervals," *International Journal of Production Economics*, vol.101, pp.286-297, 2006.

[19] Y. K. Chen, C. Y. Chen, and K. C. Chiou, "Cumulative conformance count chart with variable sampling intervals and control limits," *Applied Stochastic Models in Business and Industry*, vol. 27, pp.410-420, 2011.

[20] T. W. Calvin, "Quality control techniques for zero-defects," *IEEE Transactions on Components, Hybrid and Manufacturing Technology*, vol.6, pp.323-328, 1983.

[21] T. N. Goh, "A control chart for very high yield processes," *Quality Assurance*, vol.13, pp.18-22, 1987.

[22] M. Xie and T. N. Goh, "Some procedures for decision making in controlling high yield processes," *Quality Reliability Engineering International*, vol.8, pp. 355-360, 1992.

[23] C. W. Zhang, M. Xie, and T. N. Goh, "Economic design of cumulative count of conforming charts under inspection by samples," *International Journal of Production Economics*, vol.111, pp.93-104, 2008.

[24] M. Xie and T. N. Goh, "The use of probability limits for process control based on geometric distribution," International Journal of Quality & Reliability Management, vol. 14, pp.64-73, 1997.

[25] A. F. B Costa, " $\overline{X}$ Charts with variable parameters," *Journal of Quality Technology*, vol.31, pp.408-416, 1999.

[26] E. Çinlar, *Introduction to Stochastic Processes*, NJ: Prentice Hall, Englewood Cliffs, 1975.